Article

Wavelength Redistribution and Color Purification Action of a Photonic Crystal

Enrico Bovero, and Frank C. J. M. Van Veggel

J. Am. Chem. Soc., **2008**, 130 (46), 15374-15380 • DOI: 10.1021/ja803477h • Publication Date (Web): 22 October 2008

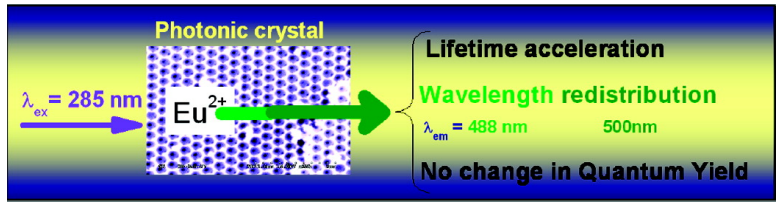

More About This Article

Additional resources and features associated with this article are available within the HTML version:

- Supporting Information
- Access to high resolution figures
- Links to articles and content related to this article
- Copyright permission to reproduce figures and/or text from this article

View the Full Text HTML

J|A|C|S
ARTICLES

Published on Web 10/22/2008

Wavelength Redistribution and Color Purification Action of a Photonic Crystal

Enrico Bovero and Frank C. J. M. Van Veggel*

Department of Chemistry, University of Victoria, P.O. Box 3065, Victoria BC, Canada, V8W3V6.

Received May 9, 2008; E-mail: fvv@uvic.ca

Abstract: Currently, photonic crystals are attracting a lot of interest because of their ability to harvest light from a device into specific directions and wavelengths. In this work we have proven the theoretical prediction that in the case of an emission overlapping with the photonic stop band, the intensity is redistributed at different wavelengths. This prediction has two major consequences: (i) the total QY remains the same and (ii) the intensity increases just outside the band gap. In our case, Eu^{2+} is the responsible emitter in a hybrid material based on GaN on silica, which has a fairly broad emission with its maximum at 500 nm. The GaN and Eu^{2+} were placed inside an inverse opal of silica (air voids in silica matrix). The size of the holes in the different samples was varied between 300 and 600 nm, in order to tune the stop band in different positions with respect to the Eu^{2+} emission. The measured quantum yield was constant for the different samples at about 5%, the lifetime of the Eu^{2+} increased in the forbidden range, and its emission intensity was squeezed toward the side of the stop band, with a concomitant decrease of the lifetime. The enhancement of the emission intensity at a certain energy range opens new possibilities for the design of more efficient devices, providing color purification and intensification at whichever wavelength is needed.

Introduction

In the past, the most common way to control the characteristics of the electromagnetic radiation was to choose the appropriate vibronic energy level structure of the material, which was the source of radiation. Lately, more and more interest is pointed toward the pursuit of photonic materials, which are able to modify the radiation by acting on the structure of the photonic levels. Photonic crystals are promising materials from these points of view.[1,2] They are systems, in which the periodic modulation of the dielectric constant over the structure of the material generates a forbidden gap of photonic states, in a similar way as a periodic lattice of atomic potentials determines a forbidden electronic gap in semiconductor crystals.[3] The combination of Bragg scattering from the periodicity of the structure and Mie scattering resonance leads to the complete exclusion of electromagnetic modes over a continuous range of wavelengths. If the periodicity of the system is not perfect or the contrast in the dielectric constant $\varepsilon(r)$ inside the structure is low, instead of a photonic band gap only a reduction of density of states (DOS) is observed, which is normally called a stop band (SB).

The simplest photonic crystals are monodimensional: the periodicity of the system and hence the gap occurs just in one direction or at different wavelengths for different directions. They are employed as coatings on lenses or mirrors to modulate the reflectivity, as color changing paints and inks, etc. Two-dimensional photonic crystals are used to design optical waveguides,[4] nanocavities,[5,6] and optical fibers[7] and as low threshold lasers.[8,9] Three-dimensional photonic crystals are hard to achieve,[10,11] but they will probably open the door to optical computing.[12] These materials are attracting more and more interest also in the hope that, in the near future, photons will be able to replace electrons as information carriers in integrated microcircuits. Photons present several advantages with respect to electrons: they can travel through dielectric materials much faster, they can carry a larger amount of information, and the energy losses are also reduced because as bosons they are not as strongly interacting as electrons.[13] So far, photonic crystals have mainly been used as a tool to control the propagation of light through the material: drive it along particular directions and stop it along others.[14] The challenge now is to understand what happens at the wavelengths on the sides of the stop bands. There is still some theoretical dispute about this,[15−18] but the

(1) John, S. *Phys. Rev. Lett.* **1987**, *58*, 2486–2489.
(2) Yablonovitch, E. *Phys. Rev. Lett.* **1987**, *58*, 2059–2062.
(3) Joannopoulos, J. D.; Villeneuve, P. R.; Fan, S. H. *Nature* **1997**, *386*, 143–149.
(4) Tsuji, Y.; Morita, Y.; Hirayama, K. *IEEE Photon. Technol. Lett.* **2006**, *18*, 2410–2412.
(5) Englund, D.; Fattal, D.; Waks, E.; Solomon, G.; Zhang, B.; Nakaoka, T.; Arakawa, Y.; Yamamoto, Y.; Vuckovic, J. *Phys. Rev. Lett.* **2005**, *95*, 013904.
(6) Yoshie, T.; Scherer, A.; Hendrickson, J.; Khitrova, G.; Gibbs, H. M.; Rupper, G.; Ell, C.; Shchekin, O. B.; Deppe, D. G. *Nature* **2004**, *432*, 200–203.
(7) Kuhlmey, B. T.; McPhedran, R. C. *Phys. B: Condens. Matter* **2007**, *394*, 155–158.
(8) Noda, S. *Science* **2006**, *314*, 260–261.
(9) Sakoda, K.; Ohtaka, K.; Ueta, T. *Opt. Express* **1999**, *4*, U1–U9.
(10) Norris, D. J. *Nat. Mater.* **2007**, *6*, 177–178.
(11) Hynninen, A. P.; Thijssen, J. H. J.; Vermolen, E. C. M.; Dijkstra, M.; Van Blaaderen, A. *Nat. Mater.* **2007**, *6*, 202–205.
(12) Vats, N.; Rudolph, T. *J. Mod. Opt.* **2001**, *48*, 1495–1502.
(13) Yablonovitch, E. *Nat. Mater.* **2003**, *2*, 648–649.
(14) Fujita, M.; Takahashi, S.; Tanaka, Y.; Asano, T.; Noda, S. *Science* **2005**, *308*, 1296–1298.

10.1021/ja803477h CCC: $40.75

most credited mechanism is that the reduction of the DOS within the SB range is accompanied by an increase of DOS on the sides of the stop band.[9,19−25] This redistribution would have determinant consequences for the design of new devices able to purify and intensify the emission at certain wavelengths.

In this work we address the problem from an experimental point of view. Eu^{2+} is the responsible emitter in a hybrid material based on GaN in SiO_2,[26] which has an intense and fairly broad emission with the maximum in the blue, but tailing into the green.[27,28] Such material was shaped into an inverse opal (air voids in silica-doped matrix), in which the size of the holes in the different samples was varied between 300 and 540 nm, in order to tune the SB in different positions with respect to the Eu^{2+} emission. Beside the modifications of the lifetime, which has extensively been observed by others,[14] we observe a decrease of spontaneous emission in the range of the photonic stop band and an increase around the low energy edge of such incomplete gap, in agreement with the modification of the DOS predicted by the theory. We assume that this effect also occurs on the high energy side, but in our sample this is probably obscured by the fact that the emission decreases very steeply. For the first time to the best of our knowledge, we observe constancy in quantum yield (QY) over the whole range of the spontaneous emission. This means that for an emitter placed inside a photonic crystal, the reduction of the local density of states not only determines a redistribution of emission along different directions, but also redistribution to different wavelengths. We could name such behavior a "smart filter": it demotes certain wavelengths and promotes others without wasting intensity, as an ordinary filter would do. A change in color coordinates due to this redistribution has indeed been observed. Such an enhancement of spontaneous emission, especially toward higher energies, opens new possibilities for the design of more efficient devices, exploiting radiation at shorter wavelengths.

Theory. In order to describe the behavior of light in a photonic crystal, the solutions of Maxwell equations in a periodic dielectric medium should be considered. After simple manipulations, they can be rewritten in the form:[29]

$$\nabla \times \left[\frac{1}{\varepsilon(r)} \nabla \times H(r)\right] = \frac{\omega^2}{c^2} H(r) \tag{1}$$

in which $\varepsilon(r)$ is the dielectric function, $H(r)$ the magnetic field of the photon, ω the frequency, and c the speed of light. It is possible to demonstrate that the operator on the magnetic field is Hermitian [$\hat{\Theta} = \nabla \times 1/\varepsilon(r)$]. Therefore, eq 1 can be seen as an eigenvalue equation, and the diagonalization of $\hat{\Theta}$ can be performed completely by considering the strength and the symmetry properties of $\varepsilon(r)$. In such a way a band structure is spanned with regions of allowed wave-vectors and forbidden gaps. An important difference with respect to the case of electrons in solids is that for photons, there is nothing like a Bohr radius.[30] Therefore, the energy of the system is scalable with respect to the size and the dielectric constant, without any modifications on the shape of the spectrum. This treatment can be extended to two and three dimensions to determine the photonic band structure depending on the periodicity of the system. A rough approximation of the wavelength of the SB can be determined considering a modified version of the Bragg's law, combined with Snell's law.[31]

$$\lambda = \frac{2Sa}{m\sqrt{h^2 + k^2 + l^2}} [\phi n_1 + (1 - \phi) n_2] \tag{2}$$

where λ is the wavelength, S is a shrinkage factor, which takes into accounts the eventual shrinkage that a structure undergoes during its formation (vide infra), a is the cell's parameter, m is the order of Bragg's diffraction, n_1 and n_2 are the refractive indexes of the materials constituting the structure, and ϕ is the volume fraction of one of them, the other being the complementary $(1 - \phi)$. In the case of direct or inverse opals, where the periodicity of the system is distorted by defects, SBs are relatively broad and eq 2 is a good prediction of the SB position.

If an emitter is inserted into a photonic crystal, its spectroscopic properties are modified by the presence of the photonic band gap. The best way to describe this is considering Fermi's golden rule:[30]

$$W = 2\pi\hbar |V_{\mathrm{fi}}|^2 \rho(E_{\mathrm{fi}}) \tag{3}$$

where W is the transition rate, $\hbar$ is the reduced Planck constant, V_{fi} is the matrix element of the potential that operates between the initial and final value, $\rho(E_{\mathrm{fi}})$ is the DOS at the energy of the transition. Equation 3 shows that the probability of a transition depends on the DOS of the system. Therefore, inside the range of the photonic SB, where the DOS is reduced, W will be lower, producing a decrease in emission intensity and a lengthening of the lifetime. Outside this range or along different directions the transition probability will not be affected, but on the edges of the SB, if the DOS really increases, it would lead to an increase of the emission intensity and a decrease in the lifetime of the fluorophore located inside the structure.

Experimental Section

All the chemicals were used as received from Aldrich: tetraethyl orthosilicate, gallium nitrate (99.98%), europium nitrate (99.98%). The anhydrous ammonia gas (99.999%) used for the nitridation was purchased from Praxiar. Milli-Q water with resistance greater than 18 MΩ was used in all our experiments.

The samples were prepared starting from the vertical deposition of polystyrene beads (PBs) (Bangs Laboratories) of different sizes, depending on the desired position of the SB. A new quartz slide (Chemglass CGQ-06040-10) previously etched overnight with chromic acid was vertically soaked in a 0.3 weight % water dispersion of PBs and heated at 60 °C for about 14 h until complete evaporation. The self-assembly of the spheres into a face-centered cubic (fcc) lattice led to the formation of an opal. These opals acted as templates for the preparation of the inverse opal sample: they

(15) Zhu, S. Y.; Li, G. X.; Yang, Y. P.; Li, F. L. *Europhys. Lett.* **2003**, *62*, 210–216.
(16) Asatryan, A. A.; Busch, K.; McPhedran, R. C.; Botten, L. C.; de Sterke, C. M.; Nicorovici, N. A. *Phys. Rev. E* **2001**, *63*, 046612/1−4.
(17) Lousse, V.; Vigneron, J. P.; Bouju, X.; Vigoureux, J. M. *Phys. Rev. B* **2001**, *6420*, 201104.
(18) Vats, N.; John, S.; Busch, K. *Phys. Rev. A* **2002**, *65*, 043808/1−13.
(19) John, S.; Quang, T. *Phys. Rev. A* **1994**, *50*, 1764–1769.
(20) Bulu, I.; Caglayan, H.; Ozbay, E. *Phys. Rev. B* **2003**, *67*, 205103.
(21) Dowling, J. P.; Scalora, M.; Bloemer, M. J.; Bowden, C. M. *J. Appl. Phys.* **1994**, *75*, 1896–1899.
(22) Nishimura, S.; Abrams, N.; Lewis, B. A.; Halaoui, L. I.; Mallouk, T. E.; Benkstein, K. D.; van de Lagemaat, J.; Frank, A. J. *J. Am. Chem. Soc.* **2003**, *125*, 6306–6310.
(23) Halaoui, L. I.; Abrams, N. M.; Mallouk, T. E. *J. Phys. Chem. B* **2005**, *109*, 6334–6342.
(24) Li, Y. Z.; Kunitake, T.; Fujikawa, S.; Ozasa, K. *Langmuir* **2007**, *23*, 9109–9113.
(25) Sakoda, K. *Opt. Express* **1999**, *4*, 167–176.
(26) Mahalingam, V.; Tan, M.; Munusamy, P.; Gilroy, J. B.; van Veggel, F. C. J. M. *Adv. Funct. Mater.* **2007**, *17*, 3462–3469.
(27) Akella, A.; Keszler, D. A. *Chem. Mater.* **1995**, *7*, 1299–1302.
(28) Tsuboi, T.; Silfsten, P. *J. Phys.: Condens. Matter* **1991**, *3*, 9163–9167.
(29) Lopez, C. *Adv. Mater.* **2003**, *15*, 1679–1704.
(30) Atkins P. W. F. R. S., *Molecular Quantum Mechanics*, 3rd ed.; Oxford Univeristy Press: Oxford, 1997; p 545.
(31) Schroden, R. C.; Al-Daous, M.; Stein, A. *Chem. Mater.* **2001**, *13*, 2945–2950.

were infiltrated with a dispersion of 50 nm silica nanoparticles formed by the hydrolysis and condensation of tetraethyl orthosilicate in 1:5 ethanol solution. The pH was set at 1 with the addition of few drops of 1 N HCl. On the surface of these silica colloids, a thin shell of Eu^{3+}-doped Ga_2O_3 was grown, infiltrating the opal with $Eu(NO_3)_3$ and $Ga(NO_3)_3$ in a 1:10 ratio in water solution. The concentration of $Eu(NO_3)_3$ was 1 mM, while that of $Ga(NO_3)_3$ was 10 mM. For the infiltration, the quartz slide was horizontally immersed two times, for 3 min each time, in a 1:5, by volume, mixture of the nitrates solution and the silica nanoparticles dispersion. The homogenization of the mixture provides a simultaneous infiltration of the silica and the dopants and ensures the homogeneity of the distribution of the europium all over the structure. The formation of Ga_2O_3, the nitradation to GaN, and the reduction of Eu^{3+} to Eu^{2+} was performed in an electric furnace (Lindberg) in a single thermal cycle. The temperature was raised to 650 °C in 6 h, maintained there for 2 h, and raised further to 950 °C over 6 h. At this point, NH_3 was fluxed at a rate of 10 SCCM (cubic centimeter per minute at STP) keeping the temperature for 2 h. After that, the temperature was decreased to room temperature over 6 h. During the first step at 650 °C, the nitrates are transformed into oxides. During the second step, the oxides are transformed into nitrides and the Eu^{3+} is reduced to Eu^{2+}. As discussed in a previous paper,[26] this process leads to the formation of GaN nanoparticles on the surface of the silica. The difference in this case is that the silica was not in the form of nanoparticles, but it was a solid inverse opaline structure. At the end, the inverse opaline structure has replaced the empty spaces of the direct opal, and the polystyrene beads have been completely removed, leaving spherical voids filled with air. The two references were grown from 300 and 540 nm PBs, respectively. Such references resemble the scattering properties of the sample, but their stop bands cannot affect the photonic properties of the active ion. For the study quantum yield (QY) measurements, beside this reference, we need yet another control sample, which mimics the scattering characteristics of sample and reference at the excitation wavelength, but which does not contain an optical emitter or absorber. Such control sample was synthesized following the same procedure, but without inserting Eu^{3+} as a dopant. We tried both without any dopant and using Y^{3+} as a dopant. The results did not change. All the samples, references, and control samples that we compare in this work were rigorously grown in the same batch and in the same thermal cycle. SEM measurements were performed with a Hitachi S35000N scanning electron microscope operating at 15 kV. All the samples and references were characterized by energy dispersive X-ray spectroscopy (EDX) using a Hitachi S-3500N scanning electron microscope, operated at 20 kV and a resolution of 102 eV. Dry powdered samples were attached to the substrate using a double-sided carbon tape and mounted onto the sample holder. Each reported value is the result of three measurements in different positions. The standard deviation was calculated on the average.

Photoluminescence measurement were recorded with an 'Edinburg Instruments' FLS 920 fluorimeter. For all the measurements, the detector employed was an R928P Hamamatsu PMT, and the resolution due to the slits' aperture was 1 nm. The emission spectra of Eu^{2+} were measured exciting with a 450 W Xe arc lamp. Transmission spectra were measured with the same fluorimeter in a 180° geometry obtained by driving the light out of the fluorimeter with two optical fibers and two objectives to focus the light in and out of the sample with two Olympus 10× objectives. The lifetimes of the same ion were collected, exciting with the 355 nm harmonic line of a Quantel Nd:YAG nanosecond laser and collected with a multichannel scaling card whose time resolution was 5 ns. The lifetime values were calculated as effective lifetimes by using the formula:[32]

$$\tau = \frac{\int_0^\infty tI\mathrm{d}t}{\int_0^\infty I\mathrm{d}t} \tag{5}$$

where τ is the lifetime, t is the time, and I the intensity. Each decay was considered until the intensity reaches 1% of the initial intensity. The color coordinates were determined from the Tristimulus values calculated by the integration of the spectra after the application of the color matching functions, which account for the human eye sensitivity. The absolute QY was determined using an integrating sphere (Edinburgh instruments, 150 mm in diameter coated with barium sulfate).[33] All the samples and references were placed in a cuvette inside the integrating sphere. The geometry of the measurement was 90°, and a baffle was placed beside the sample on the emission monochromator side, to ensure that light directly scattered from the sample could be collected before reflecting on the walls of the sphere. The reason is that a direct reflection could compromise the measurement because the samples could scatter light differently along different directions. The QY was calculated using the formula:

$$\mathrm{QY} = \frac{\int I_{\mathrm{E}}(\bar{\nu})\mathrm{d}\bar{\nu}}{\int I_{\mathrm{S-C}}(\bar{\nu}) - \int I_{\mathrm{S-S}}(\bar{\nu})\mathrm{d}\bar{\nu}} \tag{4}$$

where QY is the quantum yield, I_{E} is the emission intensity, $I_{\mathrm{S-C}}$ and $I_{\mathrm{S-S}}$ are the intensities of the light scattered from the control sample and from the sample, respectively, and $\bar{\nu}$ is the wavenumber. Hence eq 4 expresses the ratio between the number of photons emitted (numerator) versus the number of photons absorbed (denominator). The electron paramagnetic resonance (EPR) spectrum was collected on a Brucker EMX instrument operating in the X-band (9.443 GHz) at 115 K.

Results and Discussion

The growth method for the samples was pretty straightforward but necessitated a meticulous optimization, in order to maximize the quality of the opal. For instance, the concentration of the polystyrene bead (PB) dispersion and the temperature of the oven, which determined the duration of the evaporation, were critical for a uniform coating of the quartz slide. In particular, a slow evaporation (2 days) was preferable. The concentration was proportional to the thickness of the coating. A thick coating was generally uneven and not functional for optical transmission measurements. On the other hand, a too thin coating was not uniform over the area of the slide and the quality of the face-centered cubic (fcc) structure was low. The best compromise was given by optimization of the concentration, which was just enough to cover the slide completely. Any attempt to increase the thickness resulted in a decrease of the quality of the structure, a wavy profile of the layer and a thickness step at about half of the slide's height due to a natural temperature oscillation and a sudden concentration increase. Another fact that influenced the quality of the opal was the size of the beads: the smaller the beads, the easier it was to get a good quality structure. In particular, it was fairly easy to obtain good quality opals with PBs smaller than 800 nm. If the size of the beads exceeds 900 nm, the structure of the opal and the intensity of the SB start to decrease sensitively. Figure 1a is a picture of an opal made from 400 nm PBs taken from an optical microscope on a 10× magnification. Some longitudinal lines are observed on the layer, but the quality of the fcc structure is confirmed by the intensity of the stop band in the transmission spectrum measured perpendicular to the 111 planes of the lattice (Figure 2, dotted line). The barycenter of the stop band in the spectrum matches

(33) deMello, J. C.; Wittmann, H. F.; Friend, R. H. *Adv. Mater.* **1997**, *9*, 230–232.
(32) Nakazawa, E. Phosphor Handbook; CRC Press: Boca Raton, 1999; p 101

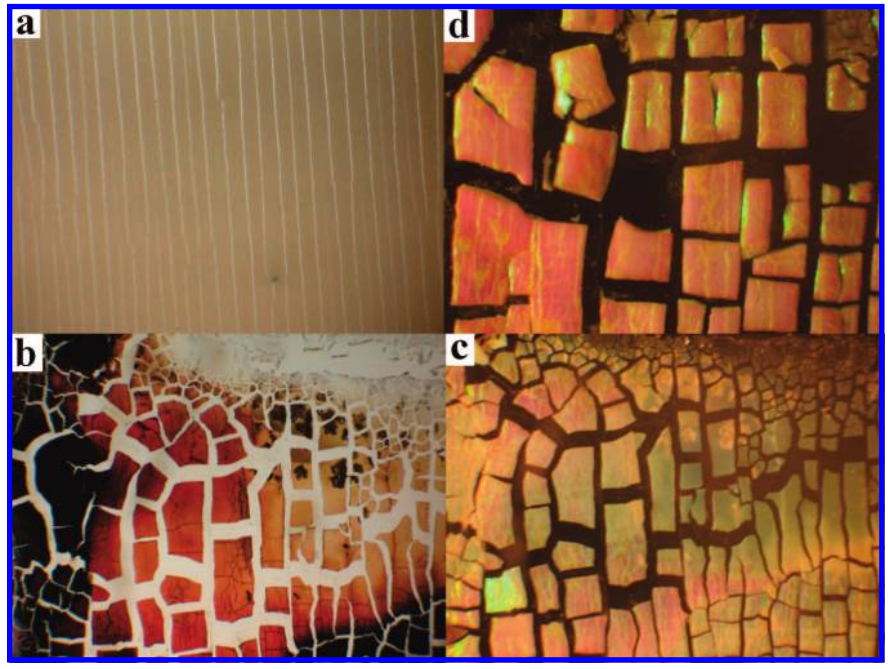

Figure 1. Digital images of the direct and inverse opals. (a) 10× magnification of a direct opal made of PBs. (b) 40× magnification of Eu^{2+}-doped silica inverse opal in transmission mode. (c) 40× magnification of Eu^{2+}-doped silica inverse opal in reflection mode. (d) 100× magnification of Figure 1c.

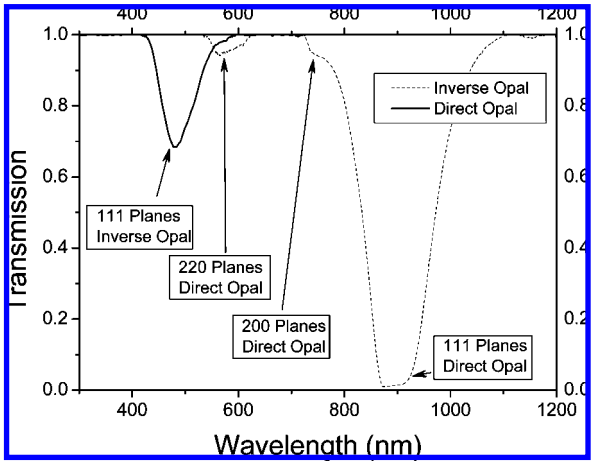

Figure 2. Transmission spectra of the direct and inverse opals made of 400 nm PBs. The assignment of the stop bands based on the planes responsible for them is in the graphic.

the expected value calculated from eq 2. Other stop bands corresponding to the 200, 220, and 311 series of planes are much less intense and negligible for our purposes. For the preparation of the inverse opals, the number and duration of each immersion was optimized at 3 min after many attempts, in order to have the most copious infiltration and the lowest possible damage to the lattice. The infiltration was driven by capillary forces in the convex structure, and it was particularly effective as proved by the result shown in Figure 3a. A constant 2 μm thickness of the sample can be derived from the scanning electron microscopy (SEM) images in Figure 3b−d, where the number of layers can be counted at the extremities of the sample and in the middle (Figure 4a and 4b, respectively). These figures also confirm the quality of the infiltration, which does not lead to any accumulation of silica on top of the inverse opal structure. The SEM images are slightly hazy because of some charging during the measurements.

The opalescent effect on the coloration of these samples is very strong: in the regions where they are not damaged, they assume the color corresponding to the position of the stop band, when the light incides from the same direction of the observer, and the complementary color of the stop band, when the light comes from the opposite direction of the observation. Figure 1b−d shows the intensity of the effect. Obviously the infiltration of the opal damaged the coatings a bit: in some parts it came off completely, and generally it was fragmented in "small islands" of roughly 0.1 × 0.2 mm. The reduced intensity of the stop band of the inverse opals observed in the transmission spectra is thus due to this fragmentation combined with the size of the beam (∼0.2 mm) used in the measurements. The transmittance of 70% observed in Figure 2, is hence an average transmittance over the whole irradiated area of the slide and therefore an underestimation of the real effect in these materials because some light is not passing through the sample. The shift in the position of the stop band passing from the opal to the inverse opal, according to eq 2, is mainly due to a shrinkage occurring during the thermal cycle. The voids are normally between 30 and 40% smaller than the PBs employed. Factor S in eq 2 takes into account this shrinkage.

For this kind of experiment, the choice of the reference is of fundamental importance. In our particular case we need two references: one to check the effect of the stop band on the Eu^{2+} emission and one to be used as control sample for the determination of the absolute QY. The best one to study the effect of the stop band is an inverse opal grown in the same way as the sample, doped with Eu^{2+}, but starting from a different size of PB in order to have the stop band outside the Eu^{2+} emission. Figure 4a shows the transmission spectra of the inverse opals compared with its two references. The sample grown from 400 nm PBs and the references grown from 300 and 540 PBs present stop bands at 477, 325, and 662 nm, respectively. The resulting shrinkage is 40% for the sample and the 325 nm reference and 35% for the 662 nm reference. The

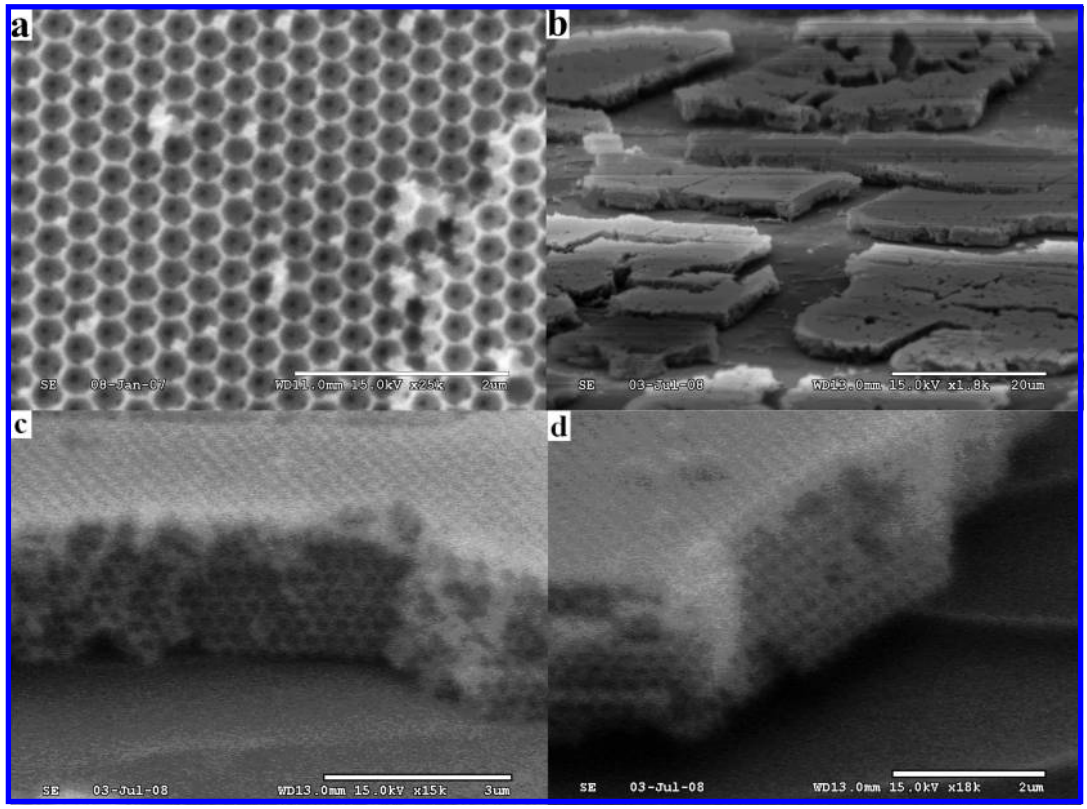

Figure 3. SEM image of the Eu^{2+}-doped inverse opal. Figure 3a shows the surface with a 90° angle of incidence. Figure 3b−d are under a 60° angle and show the thickness of the inverse opal. The scale bar measures 2, 20, 3, and 2 μm in Figure 3a, 3b, 3c, 3d, respectively.

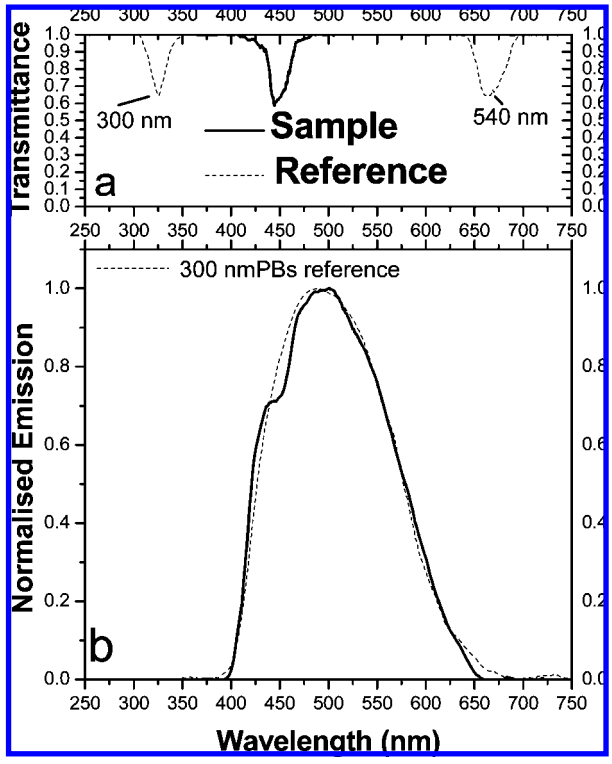

Figure 4. (a) Transmission spectra and (b) emission spectra of sample (solid line) and references (dotted line). For the references, the size of the initial PBs used for the preparation of the samples is indicated on the transmission spectra.

shrinkage seems to be higher for smaller particles/holes; this trend was confirmed in all the samples measured.

Each sample and reference underwent elemental analysis by means of energy dispersive X-ray spectroscopy (EDX). The ratio between europium and gallium was 9.4 ± 0.7%, 10.3 ± 0.8, and 9.8 ± 0.7 in the sample, the reference grown from 300 nm PBs, and the one grown from 540 nm PBs, respectively. The amount of gallium with respect to silica was about 10%. These ratios are very close to the ratios used in the experiments.

The clearest evidence of the presence of Eu^{2+} in the sample comes from the broad and intense emission corresponding to the de-excitation of the t_{2g} level of the $4f^6 5d$ configuration to the ground level $^8S_{7/2}$. This band is centered at around 500 nm, but we observed that its position changes sensitively as the NH_3 flux changes during the nitradation. For these reasons, in this work, whenever we compare samples of different size and different positions of stop band, these samples have been grown together undergoing the infiltrations in the same Petri dish and the same thermal cycle. Otherwise, differences could be due to slightly different pressures of NH_3 in the cylinder from one day to another, etc. Another confirmation of the presence of the Eu^{2+} came from the electron paramagnetic resonance (EPR) measurements (Figure S1, Supporting Information). A step that occurs between 320 and 340 mT is typical of Eu^{2+};[34−37] its broadness is due the random orientation of the sample, and it is in accordance with the results we obtained in previous work.[26]

(34) Morris, R. V.; Haskin, L. A. *Geochim. Cosmochim. Acta* **1974**, *38*, 1435–1445.
(35) Schweizer, S.; Corradi, G.; Edgar, A.; Spaeth, J. M. *J. Phys.: Condens. Matter* **2001**, *13*, 2331–2338.
(36) Kataev, V.; Khaliullin, G.; Michels, G.; Huhnt, C.; Hollandmoritz, E.; Schlabitz, W.; Mewis, A. *J. Magn. Magn. Mater.* **1994**, *137*, 157–166.
(37) Rey, J. M.; Bill, H.; Lovy, D.; Hagemann, H. *J. Alloys Compd.* **1998**, *268*, 60–65.

We never had problems observing the presence of the stop band in transmission spectra, but in order to be able to observe it in emission we had to refine the quality of the structure meticulously. Part of the reason is due to the angle of measurement: in transmission spectroscopy the geometry of the measure is 180° and perpendicular to the 111 series of lattice planes, which is the direction in which the effect of the stop band is more intense. On the other hand, in emission spectroscopy the geometry of the measure was 90°, and the angular information was lost because a big portion of the emitted light was collected by the lens on the excident beam. For this reason, the stop band seen in emission is just an average effect over several different angles. Figure 4b clearly shows the presence of the stop band as a dent at about 447 nm. The position of the stop band is reproducible in different samples because it depends on the size of the initial polystyrene beads (Figures S2 and S3, Supporting Information). On the other hand the position of the emission maximum changes from growth to growth because it depends on the ammonia flux. In each experiment the ammonia flows for more than 8 h, and small uncontrollable differences in the intensity of the flux from one experiment to the other lead to a different position of the emission maximum of Eu^{2+}, resulting in different relative positions with respect to the stop band. We tried to optimize the characteristics of the sample having the stop band on the long energy side of the emission maximum; nevertheless, the best sample that was obtained presented the stop band on the high energy side probably because the most intense stop band is obtained starting from small beads.

The emission of the reference grown from 300 nm PBs is superimposed on the same graph. The emission of the reference grown from 540 nm PBs is not reported because it is essentially the same. The parallelism with Figure 4a on top confirms that the stop bands on the references are outside the Eu^{2+} emission band, and, as expected, they do not affect its density of states. In order to facilitate the comparisons between the positions of the bands' maxima, the spectra have been normalized. Therefore, we cannot compare the relative intensities, but just the shape of the spectra. The original intensities before normalization could not be compared either, because the amount of material excited in different samples is not necessarily the same. In the literature a large number of papers can be found dealing with the orientational redistribution of light by photonic crystals.[14,38−45] However, it is hard to find clear evidence of the redistribution in wavelength, which is however expected from theory.[9,15−25] The shift in the emission maximum from 487 to 496 nm, shown in Figure 4b with respect to the samples with the stop band outside of the Eu^{2+} emission, confirms this expectation. Another confirmation of this shift comes from the color coordinates[46] calculated from the emission spectra of the sample ($x = 0.242$, $y = 0.371$) and the 300 nm ($x = 0.238$, $y = 0.367$) reference.

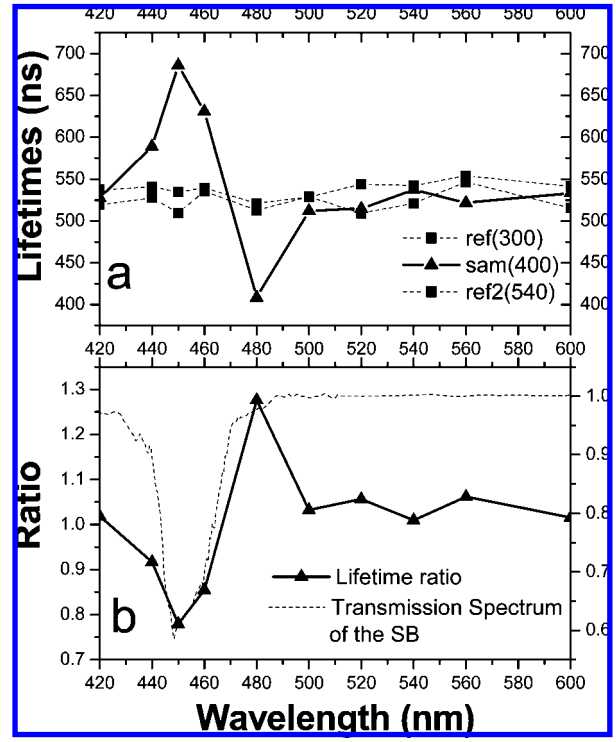

Figure 5. (a) Eu^{2+} lifetimes at different wavelengths, λ_{ex}: 355 nm. (b) Ratio between the reference and the sample; the transmission spectrum of the sample is superimposed.

Even more interesting is the confirmation coming from the QY measurements: the QY measured for the sample and for the references are $5.13 \pm 0.2\%$ and $4.99 \pm 0.2\%$, respectively. The error on the QY value has been determined by repeating each measurement 10 times. These QYs are smaller than the those reported in a previous work by Mahalingam et al.[26] However, an essential difference is that in our previous article we describe nanoparticles, whereas in the current work we have more a "bulk structured" material. Nevertheless, the emitter is Eu^{2+} albeit in a slightly different crystal field as evidenced by the different emission maxima. The constancy of the QY validates the theory that the wavelength redistribution is achieved without any reduction of the yield of the emission. Of course the angular redistribution is still present, but from our experiment, where all the light is collected out of the sample inside the integrating sphere, this effect is completely averaged. As a further confirmation of this intensity redistribution at different wavelengths, we checked what is actually happening on the stop band and on its edges by monitoring the lifetime, in order to have an actual picture of the reduction and increase of density of states. The decays of Eu^{2+} were not exactly monoexponential because of the nonhomogeneity of the crystal field around the Eu^{2+}. These experiments were carried out in a 90° geometry, the angular effect cannot be considered, and the stop band is again an average over several directions. This is another non-negligible contribution to the broadness of the stop band. If the density of states decreases, according top eq 3, the lifetime becomes longer. On the other side, if the density of states increases, the lifetime becomes shorter. Figure 5a indeed shows this behavior of the lifetimes at the wavelengths around the stop band. From the comparison with the same measurements on the references we

(38) Chuang, C. M.; Lu, W. B.; Su, W. F.; Lin, C. M.; Chen, Y. F. *J. Appl. Phys.* **2005**, *97*, 096104.
(39) Nair, R. V.; Vijaya, R.; Kuroda, K.; Sakoda, K. *J. Appl. Phys.* **2007**, *102*, 123106.
(40) Goncharov, A. P.; Gorelik, V. S. *Inorg. Mater.* **2007**, *43*, 386–391.
(41) Mizuhata, M.; Kida, Y.; Deki, S. *J. Chem. Soc. Jpn.* **2007**, *115*, 724–728.
(42) Florescu, M.; Lee, H.; Puscasu, I.; Pralle, M.; Florescu, L.; Ting, D. Z.; Dowling, J. P. *Sol. Energy Mater. Sol. Cells.* **2007**, *91*, 1599–1610.
(43) Nishijima, Y.; Ueno, K.; Juodkazis, S.; Mizeikis, V.; Misawa, H.; Tanimura, T.; Maeda, K. *Opt. Express* **2007**, *15*, 12979–12988.
(44) Subramania, G.; Lee, Y. J.; Brener, I.; Luk, T. S.; Clem, P. G. *Opt. Express* **2007**, *15*, 13049–13057.
(45) Khokhar, A. Z.; De La Rue, R. M.; Johnson, N. P. *IET Circuits Devices Syst.* **2007**, *1*, 210–214.
(46) Hunt, R. W. G., *Measuring Colour*, 3rd ed.; Fountain Press: 1998; p 336.

can definitely see the lengthening within the range of the stop band. On the edge of the stop band, the value at 480 nm definitely confirms the expected behavior. Figure 5b is a ratio between the lifetime of the reference grown from 300 nm PBs and the sample (the ratio with the other reference is not reported because it gives analogous values). When the ratio is close to 1, it means that the stop band has no effect on that particular wavelength. The increase and decrease of the ratio reflects the behavior of the density of states.

Employing photonic crystals in such a way it is possible to concentrate the emission intensity of an emitter on a desired range of wavelengths. By having a constant QY, the reduction in DOS in the range of the SB is accompanied by an increase of DOS and hence QY on the edge of the SB, which determines an increase of color purity of the emission. In the same way, by tuning the stop band on the low energy side of the emission band of an emitter, it would be possible to increase the efficiency of the device in the high energy range, which would be especially attractive in the ambit of the current quest for an intense emitter in the blue and at higher energies and extremely useful for a large number of applications, such as data storage, high energy lasers, photodiodes, etc.

Conclusion

In this work we experimentally observed a shift in the wavelength of the emission of an emitter by the action of a photonic crystal modifying its density of states. Its effect resembles the one of a smart filter which is able to modify the emission intensity without any loss of QY. This not only confirms the expectations coming from the theory, but it also opens the possibility to mold the intensity profile of an emitter. In particular, tuning the stop band on the long wavelength side with respect to the maximum of the emission, it is possible to increase the efficiency of a device on the blue side of the spectrum and at higher energy.[47]

Acknowledgment. We would like to thank Joe B. Gilroy, University of Victoria, for the measurement and interpretation of the EPR spectrum on our samples with Eu^{2+}. Authors are particularly grateful for the financial support received for this work from NSERC (Natural Sciences and Engineering Research Council of Canada) through the AGENO (Accelerator Grant for Exceptional New Opportunities) project, the Canada Foundation for Innovation (CFI), and the British Columbia Knowledge Development Fund (BCKDF) of Canada.

Supporting Information Available: Experimental details. This material is available free of charge via the Internet at http://pubs.acs.org.

JA803477H

(47) Almeida, R. M.; Goncalves, M. C.; Portal, S. *J. Non-Cryst. Solids* **2004**, *345−46*, 562–569.